A Pyridazine Series of α2/α3 Subtype Selective $GABA_A$ Agonists for the Treatment of Anxiety

Richard T. Lewis,* Wesley P. Blackaby, Timothy Blackburn, Andrew S. R. Jennings, Andrew Pike, Rowan A. Wilson, David J. Hallett, Susan M. Cook, Pushpinder Ferris, George R. Marshall, David S. Reynolds, Wayne F. A. Sheppard, Alison J. Smith, Bindi Sohal, Joanna Stanley, Spencer J. Tye, Keith A. Wafford, and John R. Atack

The Neuroscience Research Centre, Merck Sharp & Dohme Research Laboratories, Terlings Park, Eastwick Road, Harlow, Essex, CM20 2QR, United Kingdom

Received November 15, 2005

The development of a series of $GABA_A$ α2/α3 subtype selective pyridazine based benzodiazepine site agonists as anxiolytic agents with reduced sedative/ataxic potential is described, including the discovery of **16**, a remarkably α3-selective compound ideal for in vivo study. These ligands are antagonists at the α1 subtype, with good CNS penetration and receptor occupancy, and excellent oral bioavailability.

Introduction

γ-Aminobutyric acid (GABA), the major inhibitory neurotransmitter in mammalian brain, regulates chloride ion flux into neuronal cells by ligand gating $GABA_A$ receptors. This family of membrane spanning ion channels serve as arbiters of neuronal inhibitory tone and thereby play a crucial role in the regulation of neurotransmission in the CNS. The benzodiazepine class of anxiolytic, sedative, hypnotic, and myorelaxant therapeutic agents are known to exert their pharmacological effects through allosteric modulation of the effects of endogenous GABA on the conductance of the $GABA_A$ receptor. Since these agents have no significant effect upon the ion channel in the absence of GABA binding at its modulatory site, their mechanism of action ensures a safer pharmaceutical profile in comparison with barbiturates, for example, which may activate the channel directly. The myorelaxant/ataxic, sedative/hypnotic, and memory impairing properties of benzodiazepines are considered of clinical benefit when they are utilized in anesthesia, particularly for minor surgical procedures. However these same properties are considered a significant liability when these agents are used in the treatment of anxiety; such side effects may make it difficult for the patient to function normally while on medication and may even be considered as potentially dangerous for those who work in a mechanized environment.

The $GABA_A$ channel is composed of a pentameric assembly of protein subunits, and 19 subtypes of these subunits are known[1a] (α_{1-6}, β_{1-3}, γ_{1-3}, δ, ϵ, π, θ, and ρ_{1-3}), which may theoretically coassemble to form a plethora of structurally different but functionally competent ion pores. Speculation that these might reasonably be expected to possess different properties and distribution in various brain regions is now supported by a growing body of evidence. Fortunately, in studying the interaction with benzodiazepine (BZ) ligands, one need not consider the multitude of possible receptor subtype combinations, since only those which contain a γ2 or γ3[1c] subunit in conjunction with α1, 2, 3, or 5 seem to bind this class of agents with significant affinity. The benzodiazepine binding pocket appears to be located at the interface of γ and α subunits, with residues on both proteins making significant contributions to the active site. Since the GABA binding site requires contributions from both an α and β subunit, we therefore need only consider channels composed of α, β, and γ subtypes[1] for our purposes.

* To whom correspondence should be addressed. Tel +44 (0)1279 440000; Fax +44 (0) 1279 440390; e-mail: richard_t_lewis@btinternet.com.

The question remained as to whether it was possible to discover subtype selective BZ site ligands, and whether it would thus be possible to separate the anxiolytic from the sedative properties. Elegant studies in transgenic mice,[2] and in vivo studies with subtype selective ligands generated in our laboratories,[3] have now shown that receptors containing α1 seem to be strongly linked with the sedative and ataxic properties of BZ ligands, while α2 may be linked with at least part of their anxiolytic profile. The role of α3 in anxiolysis has recently been established.[3d] Here we report the culmination of our endeavors to develop a series of α2 or α3 subtype selective BZ ligands based on a pyridazine motif, as anxiolytic agents with reduced ataxic potential, including the discovery of **16**, a remarkably α3 selective compound ideal for in vivo study.

Results and Discussion

In our extensive search for subtype selective ligands at the BZ site, we have observed that it is generally not possible to obtain more than 10-fold binding selectivity for α2/α3 over α1.[4] While binding selectivity may be difficult to achieve via the BZ site, our observations indicate that functional selectivity is attainable. In this work, the selectivity described is functional in origin, i.e., selective efficacy. Because the BZ site is an allosteric modulatory site (vide supra), compounds which bind to it may elicit a range of different effects. Those which cause an enhancement of the potency of GABA and hence increased channel Cl^- conductance are termed agonists (more properly known as positive allosteric modulators), while those which reduce the potency of GABA are referred to as inverse agonists (negative allosteric modulators). Compounds which bind at the BZ site but which do not influence the properties of GABA on the channel are commonly termed antagonists, and since there is generally considered to be no endogenous ligand for the BZ binding site, such compounds have no functional effects, either in vitro or in vivo. We have therefore sought compounds with an antagonist profile at α1, and varying degrees of agonism at α2 and α3. A role for α5-containing subtypes in learning and memory impairment has been suggested, so low efficacy at this subtype is preferred.[5] Widely prescribed BZ ligands such as diazepam and chlordiazepoxide (CDZ) are full agonists at all these subtypes and cause maximal potentiation of GABA. The compounds described below have, in many cases, higher affinity for the BZ binding site, but are less efficacious at modulating the effects of GABA; they are therefore termed partial agonists, and their efficacy is reported as a fraction relative to the response achievable with chlordiazepoxide under the same test conditions.

10.1021/jm051144x CCC: $33.50
Published on Web 03/22/2006

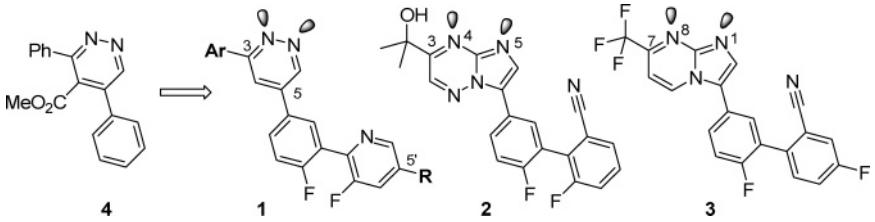

Figure 1. Consideration of structural similarity of pyridazine lead with known[7] imidazopyrimidine and imidazotriazine BZ site selective agonists.

The pyridazine series of benzodiazepine site ligands **1** described herein originated from **4**, identified by screening of the Merck sample collection, and preliminary exploratory structure−activity relationships (SAR) for this lead have been reported.[6] We were attracted by the results of these early studies, which hinted that α2 or α3 subtype selective compounds might be obtained. In addition we recognized certain structural similarities with imidazotriazine **2** and imidazopyrimidine **3** series of subtype selective GABA$_A$ ligands which we have extensively explored at Merck.[7] It was initially postulated that the adjacent nitrogens of the pyridazine core-structure might effectively mimic the disposition of the nitrogen atoms at positions 4 and 5 of imidazotriazine **2** (or the corresponding 1 and 8 positions of **3**), and this influenced the direction in which we chose to develop the SAR of this series (Figure 1). Gratifyingly, the extensive SAR which had been mapped out for the biaryl appendage in the imidazotriazine and imidazopyrimidine work[7] proved to be directly transferable into the new series and conferred similar effects upon selectivity of efficacy modulation with respect to α unit subtype when appended at the 5-position of the pyridazine core. We selected the two fluoropyridyl moieties (**1**, R = H or F) indicated in Table 1 for several compelling reasons. Generally they both afforded selective efficacy in their own right in the desired sense (but differed in that the 3,5-difluoropyridine conferred lower efficacy at all subtypes while retaining the selectivity window between them), offered structural diversity from our other series, and conveyed good pharmacokinetic (PK) properties (vide infra).

Unsurprisingly, the SAR of the 3-substituent, which crudely maps to the 3-position of the imidazotriazine (or 7-position in the imidazopyrimidine) proved to be significantly different from these other series, presumably at least partially as a consequence of alteration of the geometry and size of the heterocyclic scaffold.[8] This was regarded as advantageous in providing a structurally distinct alternative series. A pendant aryl moiety emerged as the 3-substituent of choice, conferring enhancement of affinity. The receptor was also quite tolerant to a range of substituents on this appendage, although obtrusive polar or sterically demanding substituents at the para position tended to be detrimental. Selected compounds of interest for their selective efficacy profile are listed in Table 1. All show good (but relatively unselective) binding affinity for α1, 3, and 5 subtypes.[9] Selective efficacy could be modulated by appropriate choice of substitution pattern on this moiety. Thus substitution at one or both ortho positions proved to be beneficial both for affinity and opening the window of selective α3 agonism over α1, particularly when the flanking groups possessed lone pair electron density to buttress the adjacent pyridazine nitrogen lone pair. This is suggestive of an orthogonal disposition of these two rings being optimal from an α3 selective efficacy standpoint. We favored a bias toward an electron deficient aromatic moiety from an early stage in this work because we were aware of the intrinsically high turnover of the earlier compounds[6] in liver microsomal preparations, which we routinely employed as a convenient surrogate marker of in vivo stability. The strategy utilized to optimize metabolic stability in the pyridazine series built upon the extensive knowledge of the metabolic fate of several other GABA ligands from these laboratories. The two pyridazine-5-biaryl substituents chosen from the start in opti-

Table 1. Binding Affinity and Efficacy at GABA$_A$ Receptor Subtypes

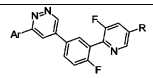

Compd. #	Ar	R	Ki (nM)[a] α1	Ki (nM)[a] α3	Ki (nM)[a] α5	Efficacy[b] α1	Efficacy[b] α2	Efficacy[b] α3	Efficacy[b] α5
6		F	-	5.6	3.8	0.02	-	0.21	-
7		H	-	0.9	0.5	0.11	-	0.31	-
8		F	-	1.7	0.7	-20%	0.20	0.40	-20%
9		F	-	3.1	1.4	0.07	-	0.42	-
10		H	0.1	0.4	0.3	-5%	-	0.24	-
11		H	0.9	5.6	7.7	-8%	0.24	0.58	-3%
12		F	3.5	8.2	5.6	-7%	-	0.41	-
13		H	0.8	3.2	3.0	-7%	-	0.39	-
14		F	1.8	6.3	6.0	-3%	0.28	0.39	-5%
15		H	0.5	2.0	2.8	-0.8%	0.43	0.70	0.40
16		F	1.5	8.5	12.1	-7%	0.12	0.44	0.01
17		F	2.6	5.0	5.1	-9%	0.36	0.40	0.14
18		H	0.5	1.4	2.4	-30%	-	0.40	-
19		F	0.4	1.7	3.2	-26%	-	0.17	0.14

[a] K_i values for benzodiazepine sites on stably transfected GABA$_A$ receptors αxβ3γ2 (x = 1, 2, 3, or 5). Inhibition curves were carried out using receptors labeled with [^{3}H]Ro15-1788 at a concentration of approximately twice the K_d. K_i values were calculated according to the Cheng−Prussof equation. Data shown are mean values for three to six determinations.[3] Efficacy measured at GABA$_A$ receptors stably expressed in L(tk$^-$) cells using whole cell patch clamp recording and represents the effect of the test compound on the current produced by an EC$_{20}$-equivalent of GABA.[3] [b] Efficacy is expressed relative to the full agonist chlordiazepoxide (CDZ) (relative equivalent efficacy = 1.0), except where a percentage value is shown, which represents a direct percent modulation of the EC$_{20}$ control. Values are the mean from at least four independent experiments. Negative values reflect a reduction in the GABA EC$_{20}$ induced chloride current and indicate inverse agonist responses; these are reported as a percentage modulation since expression of inverse agonism relative to an agonist standard is inappropriate.[3]

Table 2. Liver Microsomal Turnover, Selected Pharmacokinetic Parameters, and Rat In Vivo Receptor Occupancy Data

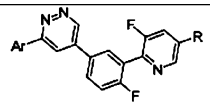			Microsomal Turnover[a] % (±5)			Rat PK[b] Parameters			Dog PK[b] Parameters			Rhesus PK[b] Parameters			Rat In-vivo receptor Occupancy[c]
Compd. #	Ar	R	Rat	Dog	Man	Clp ml/min/kg	$T_{1/2}$ (h)	F %	Clp ml/min/kg	$T_{1/2}$ (h)	F %	Clp ml/min/kg	$T_{1/2}$ (h)	F %	Occ_{50} (mpk po)
6		F	7	20											-
7		H	11	34											-
8		F	22	31	8	30	2.2	11							3
9		F	13	18	<5										4.6
10		H	19	24	13										-
11		H	17	8	8	91	0.8	5							7.2
12		F	23		<5										15.3
13		H	9	9	9										<0.2
14		F	5	4	3	59	1.6	50	17	3.9	72	6	8.4	46	0.22
15		H	<5		6	3	10	100							0.09
16		F	3	8	3	1.3	53	88	3.9	15	40				0.52
17		F	4	0	7										0.7
18		H	3	2	5										0.5
19		F	<5		<5										<0.2

[a] Microsomal turnover data were obtained by incubation of the test compound (and diazepam as a control compound) at 1 μM concentration with liver microsomes pooled from a number of individuals, at a protein concentration of 0.5 mg/mL for 0.25 h. Concentration of test compound remaining after incubation was determined by LC/MS/MS analysis. Turnover values are the mean of three determinations, with a standard deviation of </= 5% for the values quoted.[3] [b] Determined in six animals, three dosed iv and three po. [c] Rat in vivo receptor occupancy was measured with [^{3}H]Ro15-1788 according to the published protocol[3] and is the mean of three to six independent determinations.[12]

mizing this series were well-known to us as very resistant to microsomal metabolism from our study of the imidazotriazine series.[7d] Any remaining metabolic weak spots were therefore likely to reside in the 3-arylpyridazine moiety. Pyridazine N-oxidation was a strong suspect, which might be ameliorated by appending an electron-withdrawing aromatic moiety at the 3-position. The 31% turnover of **8** in dog microsomal incubation was reduced to just 2%, for its pyridazine-2-oxide derivative **5a**, (and 10% for **5b** Figure 2). More strongly electron-withdrawing 3-substituents, such as difluorophenyls, **9** and **10**

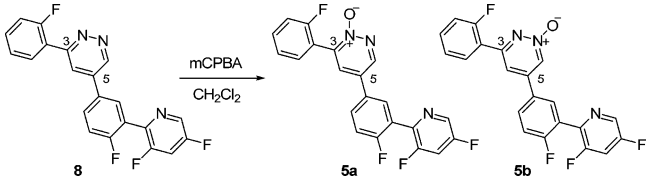

Figure 2. Synthesized pyridazine *N*-oxides **5** are significantly more resistant to liver microsomal turnover in vitro than is parent pyridazine **8**.

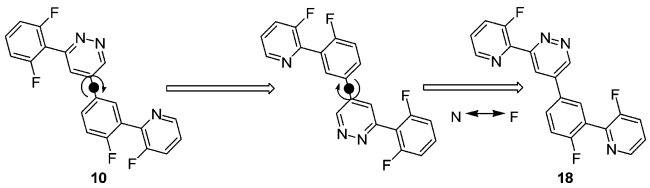

Figure 3. Illustration of the conceptually pseudo-symmetric nature of ligand structure resulting from consideration of nitrogen/fluorine interchangeability.

had excellent affinity and interesting efficacy profiles (Table 1), but microsomal turnover, although much improved over earlier compounds, was still considered to be too high, particularly in dog (Table 2).

The second conceptual approach, which afforded a solution to this problem, arose from a consideration of the pseudo-symmetric nature of the molecular structure (Figure 3). In our exploration of the SAR of several series of BZ ligands, we have encountered a reasonably general observation that a ring nitrogen may be successfully replaced with a pendant fluoro substituent or vice versa. The 5-appended fluorophenyl-fluoropyridine biaryl moiety is metabolically stable, and the arylpyridazine motif is superficially quite similar to it when nitrogen/fluorine transposition is factored in. This concept is most apparent in the comparison of compound **10** with **18**, as shown in Figure 3. If the enzymes responsible for the metabolism recognize only a portion of the entire molecule, i.e. a biaryl motif, then it might conceivably be possible to render both biaryl moieties similarly stable. This was borne out in practice. Hence, replacement of the difluoroaryl of **10** with 3-fluoropyridine **18** gave improved microsomal stability in rat, dog, and human (Table 2), with turnover reduced from around 20% in rat and dog for **10** to less than 5% for **18**. Further exploration of this SAR led to discovery of a selection of compounds with good microsomal stability (Table 2) and very interesting efficacy profiles (Table 1). It is interesting to compare, for example, the efficacy profiles of compounds **9** and **12**; **10** and **18**; and **14**, **16**, and **17**.

The somewhat poorer rat PK profile of compounds bearing a 4-pyridyl motif was traced to a propensity for pyridine *N*-oxide formation (**20**, Figure 4) in this species, confirmed in the case of **14** by comparison of its metabolite profile with an authentic standard.[10] Relocation of the pyridine nitrogen to the ortho position, as in **16**, circumvented this route and accounts for the exceptional stability and half-life of this compound in rat. This metabolic pathway does not appear to be quite so predominant in the other species studied. While compounds which are highly turned over by liver microsomes are very likely to have poor PK, low turnover is not necessarily indicative of good PK. It is clear from these studies that for this series, the rat microsomal turnover is not particularly well correlated with in vivo stability. It served a very useful function in assisting the optimization process, but should not be relied upon in isolation.

Compound **14** has acceptable PK properties in three safety species, and with low intrinsic clearance in dog, monkey and human liver microsomes, is predicted to have good PK

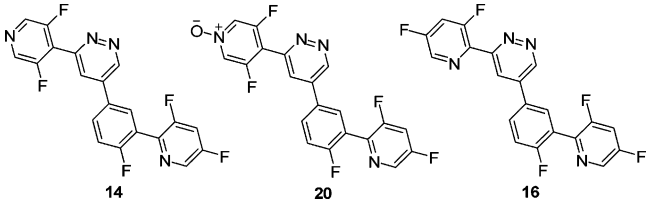

Figure 4. Circumventing the principal route of metabolism in rat. Pyridine *N*-oxide **20** is the major characterized metabolite of **14** in vitro. The 2-pyridyl isomer **16** is resistant to microsomal turnover in vitro.

properties in man. It is possessed of an interesting selective efficacy profile, being a clean antagonist at α1 and α5, and weak-to-moderate partial agonist at both α2 and α3 subtypes (Figure 5). The compound occupies the BZ receptor very effectively in rat after po dosing,[11] with an Occ_{50} of 0.22 mpk[12] (milligrams per kilogram), at a plasma concentration of 38 nM. In the rat plus-maze[11] it was anxiolytic at a minimum effective dose of 0.3 mpk po, corresponding to 56% receptor occupancy[12] (Figure 6). Furthermore, compound **14** was fully effective in the squirrel monkey conditioned emotional response (CER) paradigm, a more stringent test of anxiolytic potential.[11] In the presence of a stimulus associated with shock (conditioned stimulus (CS)), the response rate at 1 mpk po was 60% of that observed in the absence of the CS (compared with a 10% response rate in vehicle treated control animals), a significant anxiolytic response. At doses between 1 and 10 mpk (the highest studied, which corresponded to an 80% release rate) no overt signs of ataxia or sedation were observed. In contrast, a similarly therapeutic dose of diazepam (1 mpk, resulting in a 68% release rate) causes obvious behavioral disruption in this assay. In the mouse rotarod assay,[11] a measure of ataxia, the compound had no significant effect at 10 mpk po (corresponding to 97% receptor occupancy[12]) in either the absence or presence of a subthreshold dose of ethanol. It is therefore apparent that the anxiolytic properties may indeed be separated from the ataxic effects in an appropriately subtype selective compound, and that its effects are not as prone to potentiation by ethanol as traditional unselective BZ full agonist anxiolytic agents. As such, it will be of significant interest to observe its properties in man[13] where a more accurate gauge of side effect profile, including sedative and cognitive effects, may be made. As a clean α5 antagonist, one might expect less memory disruption or cognitive impairment to be evident.

Compound **15** is the most potent of the α2/α3 selective agonists discovered in this series. Structurally it differs from **14** in two respects. Fluorine and nitrogen have been transposed in the 3-substituent leading to a much improved rat PK profile (Table 2), with low clearance translating to a 10 h half-life in this species. The second point of variation is deletion of a fluorine (R = H, Table 1) on the other pyridine substituent, which results in significantly increased α2/α3 efficacy (∼0.2 elevation at both subtypes, cf. close analogue **16**, Figure 5). Gratifyingly, it is also devoid of efficacy at α1, but has agonism at α5 subtypes. The compound is a potent anxiolytic in the rat plus-maze at 0.1 mpk po, which corresponds to 57% receptor occupancy (Figure 6, Occ_{50} 0.09 mpk). It showed no significant effect at 3 mpk po in the mouse rotarod ataxia assay, with no significant impairment in the presence of ethanol at doses which gave 90% receptor occupancy.

Compound **16**, differing from **15** only by the presence of a 5-fluoro substituent (R = F, Table 1) has an intriguing profile, remarkable in that its only significant efficacy is through the α3 subtype, being effectively functionally silent at α1, 2, and 5 (Figure 5). In addition, with low intrinsic clearance in rat,

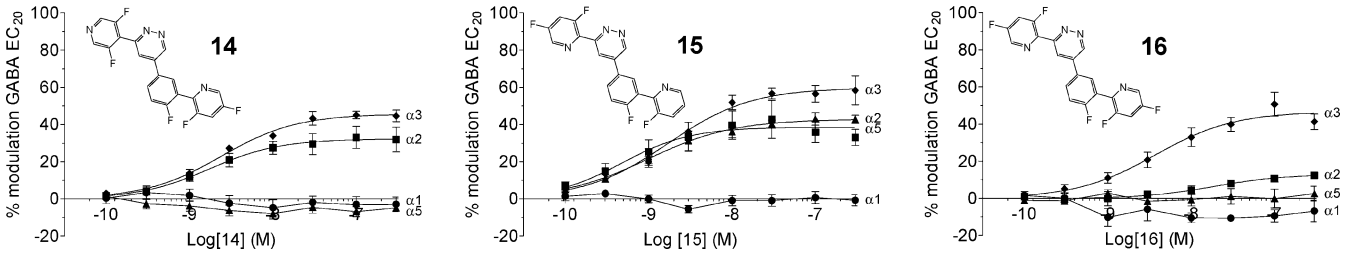

Figure 5. Efficacy profiles of **14**, **15** and **16** at human recombinant $GABA_A$ α(n)β3γ2receptors. Footnote: Efficacy profiles of **14**, **15**, and **16** at human recombinant $GABA_A$ receptors comprising β3, γ2, and either an α1, α2, α3, or α5 subunits as measured using whole-cell patch clamp electrophysiology. A potentiation of the current produced by an EC_{20}-equivalent of GABA represents benzodiazepine site agonism whereas an attenuation (negative modulation) corresponds to inverse agonism. Values shown are mean ± SEM (n = 4−6/data point).

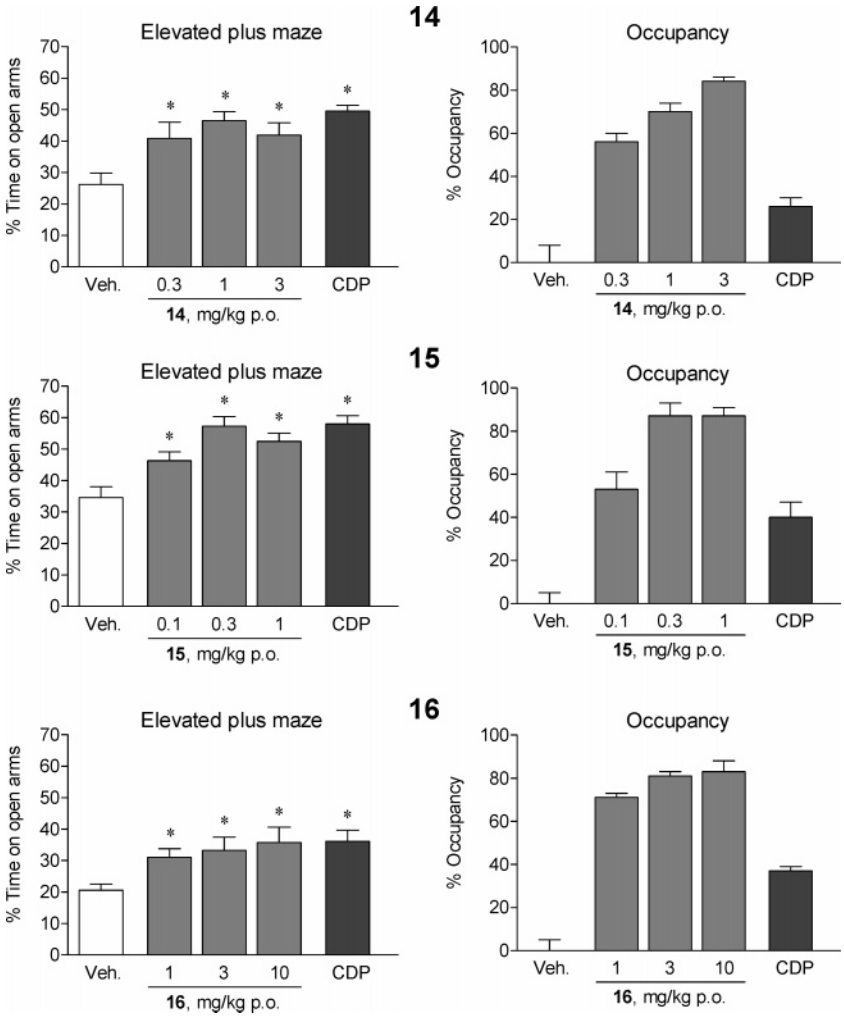

Figure 6. Anxiolytic effects (elevated plus maze), and benzodiazepine binding site occupancy of **14**, **15**, and **16** following oral dosing to rats. Footnote: Rats were dosed with either vehicle (0.5% methyl cellulose), pyridazine **14**, **15**, or **16** or, as a positive control, the nonselective full agonist chlordiazepoxide (CDP, 5 mg/kg ip). Thirty min later animals were placed on the elevated plus maze and the time spent on the open arms was recorded as an index of anxiety. A significant increase in time on the open arms relative to vehicle treated animals (*, $p < 0.05$) represents anxiolytic-like activity. Following completion of the plus-maze trial, a subgroup of rats were taken and occupancy measured using an in vivo [^{3}H]Ro 15−1788 binding assay. Compounds **14**, **15**, and **16** all produced dose-dependent occupancy with respective ED_{50} values of 0.22, 0.09, and 0.52 mg/kg. Values shown are mean ± SEM (n = 16−18/group, plus-maze experiment, and n = 5−10/group, occupancy assay).

dog, and human liver hepatocytes, it is also predicted to have good PK properties in man. In the rat plus-maze it was anxiolytic at a minimum effective dose of 1 mpk p.o, corresponding to 71% receptor occupancy[12] (Figure 6, Occ_{50} 0.52 mpk). The compound is apparently less potent in this assay than **14**, presumably because its efficacy is now mediated predominantly through the α3 subtype, which is of relatively low abundance in the CNS. This result is of particular interest because it offers further evidence of a role for the α3 subtype in anxiolysis.[3d] Other properties and benefits pertaining to this efficacy profile await exploration.

Chemistry

An efficient five-step synthesis of key chloropyridazine intermediates **26a**,**b** was developed (Scheme 1), which proceeded with an overall yield of 40% **26b** to 50% **26a** based upon the starting halopyridine. Thus coupling of 2-fluorophenylboronic acid with the requisite halopyridine proceeded

Scheme 1. Synthesis of Key Coupling Partner Chloropyridazine **26**[a]

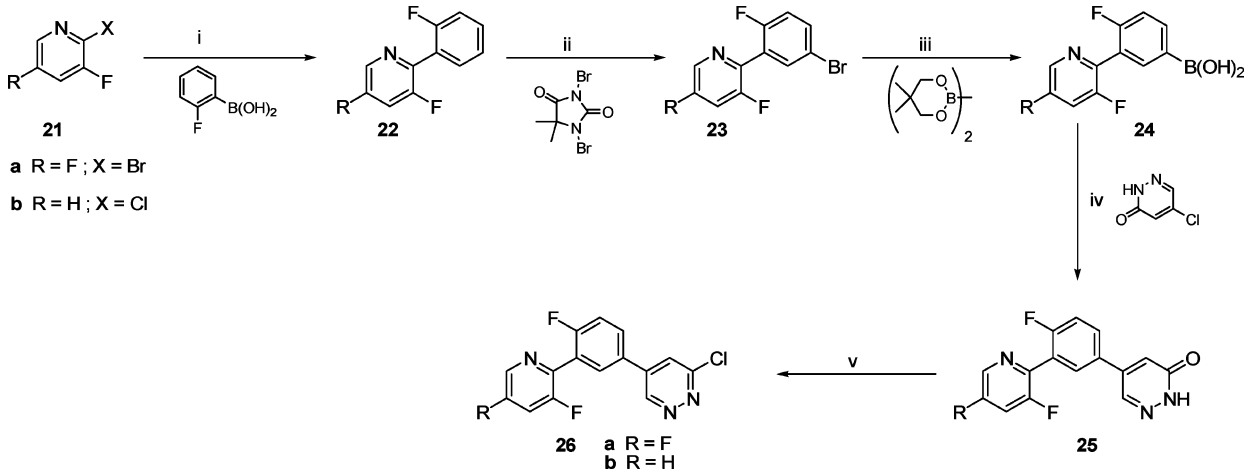

[a] Reagents and conditions: (i) $Pd_2(dba)_3$, t-Bu_3P, KF, THF, 55 °C; (ii) CH_3CN, H_2SO_4; (iii) (a) $Pd(dppf)Cl_2$, KOAc, dioxane, 80 °C, (b) HCl; iv) $Pd(dppf)Cl_2$, Na_2CO_3, dioxane, 85 °C; (v) $POCl_3$, 75 °C.

Scheme 2. Routes to Selectively Metallated 3,5-difluoropyridine[a]

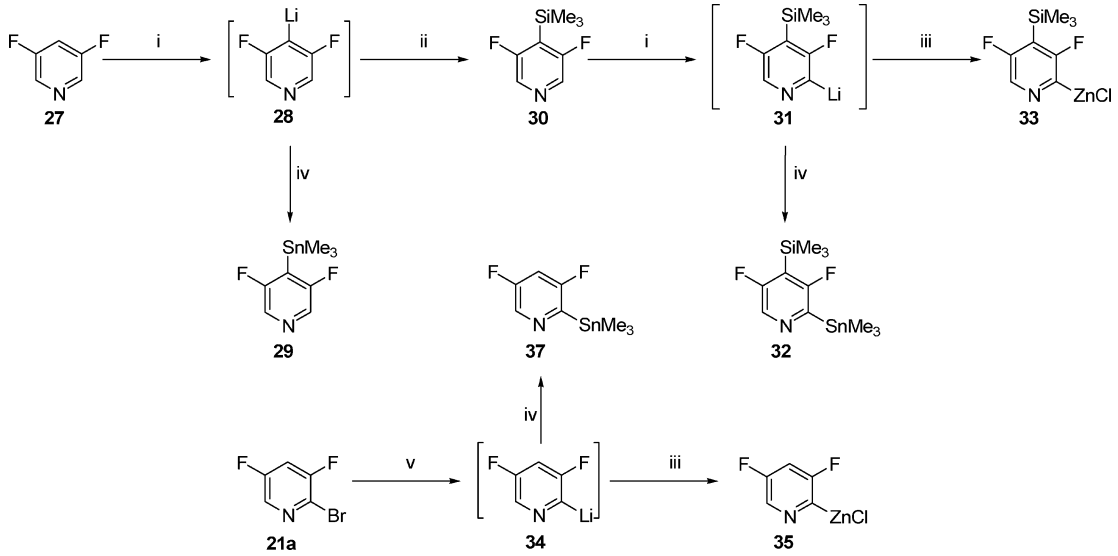

[a] Reagents and conditions: (i) n-BuLi, TMEDA, diethyl ether, −78 °C; (ii) TMSCl; (iii) $ZnCl_2$; (iv) Me_3SnCl; (v) n-BuLi, THF, −78 °C.

smoothly under the Fu conditions.[14] Addition of a small quantity of water was found to significantly enhance the rate of this reaction, presumably by rendering the potassium fluoride more soluble and therefore facilitating boron-ate formation. Bromination of **22** with dimethylhydantoin dibromide in the presence of acid[15] afforded bromide **23**. Some bis-bromination was observed if the reaction was run for a longer period, but could be avoided by careful control of reaction time. Palladium-catalyzed borylation[16] was efficient. It was found that although the boronate ester could be isolated, a base extraction followed by acidic hydrolysis afforded clean boronic acid without recourse to chromatography, a process amenable to large scale preparation of **24**. Suzuki coupling with 5-chloropyridazin-3-one,[6] followed by brief exposure to hot phosphorus oxychloride afforded **26a** or **26b**. All these transformations could be performed at scale to access significant quantities of material.

The remaining 3-aryl appendage could be introduced into **26** under a variety of different coupling protocols depending on availability of precursors. On a small scale, the pyridines **11** to **19**, and also compound **17**, were prepared by Stille cross-coupling of the corresponding stannanes, or by Negishi coupling of the arylzinc, both species being readily accessible from the corresponding lithiated pyridine (Scheme 2). The Negishi protocol is preferable on a larger scale, as the final compound is easier to render free from heavy metal contamination. The regioselective deprotonation of functionalized pyridines has been the subject of some excellent studies.[17] 3,5-Difluoropyridine **27** may be cleanly deprotonated at the 4-position to afford thermodynamically more stable anion **28** which may be readily transformed into the appropriate Stille or Negishi coupling partner as indicated in Scheme 2. Silylation of **28**, followed by a second deprotonation, allows access to **32** or **33** in a controlled manner. This procedure could be performed either stepwise with isolation of compound **30**, which is to be preferred on a larger scale; alternatively **28** could be transformed into **32** in one pot without isolation of intermediate **30**. (The kinetic deprotonation of **27** at the 2-position under the Queguiner conditions was difficult to control and led to some scrambling of regiochemistry.) The silane was readily cleaved by warming with 5 N aqueous HCl after coupling **32** to **26**. For the corresponding Negishi reaction of **33**, cleavage of the silane occurred under the coupling conditions, and for a large scale synthesis of **16** was completed by including a KF treatment in the workup. The Stille coupling could also be performed in the reverse sense, via in situ preparation of stannane **36** (Scheme 3), and was the method of choice for compounds **10** and **17**.

Scheme 3. Coupling Strategies forAssembly of the Completed Ligands[a]

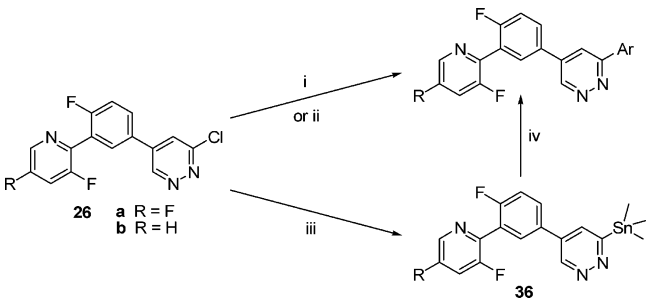

[a] Reagents and conditions: (i) $ArB(OH)_2$, $Pd(Ph_3P)_4$, Na_2CO_3, dioxane, (85 °C thermal or 150 °C microwave); (ii) $ArSnR_3$, LiCl, CuI, $Pd(Ph_3P)_4$, dioxane, 100 °C; (iii) $Me_3SnSnMe_3$, $Pd(Ph_3P)_4$, LiCl, dioxane, 100 °C; (iv) ArBr, $Pd(Ph_3P)_4$, LiCl, dioxane, 100 °C.

Alternatively, with the availability of bromopyridine **21a**,[18] the extreme rapidity of lithium−halogen exchange at low temperature may be exploited to give access to 2-lithio species **34**, which may be cleanly trapped at low temperature to afford Negishi and Stille partners **35** or **37**. Controlled deprotonation of 3-fluoropyridine at either 2 or 4-positions, proceeds smoothly according to literature precedent,[17] to give access to the required stannanes for compounds **11**, **12**, **18**, and **19**. Compounds **6**, **7**, **8**, and **9**, were similarly assembled from the commercial boronic acids by Suzuki coupling (Scheme 3).

Conclusions

In summary, we have designed a series of benzodiazepine site ligands with an array of attractive functional selective efficacy profiles. In particular, compounds **14**, **15**, and **16** stand out as antagonists at the α1 subtype, with good CNS penetration and receptor occupancy, and excellent oral bioavailability. It will be interesting to see how these subtype selective compounds perform, not only with regard to the sedative, myorelaxant, memory impairment, and anxiolytic properties associated with current clinically utilized unselective agents, but also whether they offer advantage in reducing such liabilities as potential to induce tolerance and dependence, abuse liability, and potentiation with ethanol. These compounds are well suited to examine the hypothesis that BZ ligands devoid of α1 efficacy will be effective treatments for anxiety disorders with fewer debilitating side effects; hopefully this will lead to more effective treatments for a range of anxiety conditions. Furthermore, a comparison of **14** with **15** may permit an examination of the role of α5 subtypes in the memory and cognitive impairment liabilities, while the remarkably selective **16** affords the opportunity of examining the pharmacology of the α3 subtype in isolation. Together these compounds are useful tools for advancing understanding of how subtly GABA fulfils its role as the major inhibitory neurotransmitter in a host of neuronal pathways in mammalian brain.

Experimental Section

Experimental Details for Biological Assays. Detailed experimental protocols for the in vitro and in vivo experiments have been published in ref 3 and references therein.

General Chemical Experimental Details. ^1H NMR spectra were recorded on Bruker AMX500 or DPX400 spectrometers. Chemical shifts are reported in parts per million (δ) downfield from tetramethylsilane as internal standard and coupling constants in hertz. Melting points were determined on a Leica Galen III hot stage apparatus and are uncorrected. Mass spectra were recorded on a Waters Micromass ZMD2000 or Micromass ZQ instrument operating in electrospray (ES) mode, as indicated. (Note that only the strongest peaks from the mass spectra are reported.) Spectra were recorded between 100 and 800 Da. Accurate mass data was obtained on a Micromass QTof micro. Elemental analyses for carbon, hydrogen, and nitrogen were performed by Butterworth Laboratories, 54-56 Waldegrave Road, Teddington, U.K. Analytical thin-layer chromatography (TLC) was conducted on precoated silica gel 60 F_{254} plates (Merck). Visualization of the plates was accomplished by using UV light and/or iodine and/or aqueous potassium permanganate solution. Chromatography was conducted on silica gel 60, 220−440 mesh (Fluka) under low positive pressure. Solutions were evaporated on a Büchi rotary evaporator at reduced pressure. Microwave reactions were performed using a Smith Synthesizer, supplied by Personal Chemistry, Uppsala, Sweden. All starting materials were obtained from commercial sources and used as received unless otherwise indicated. Purity for all target compounds was greater than 98% as assessed by NMR and HPLC.

3,5-Difluoro-2-(2-fluorophenyl)pyridine (22a). 2-Fluorobenzeneboronic acid (25.0 g, 178 mmol), 2-bromo-3,5-difluoropyridine (34.65 g, 178.6 mmol), dry THF (360 mL), potassium fluoride (34.25 g, 0.589 mol), and water (30 mL) were combined in a 2 L flask, and the mixture was degassed by vacuum/N_2 cycles. Tris(dibenzylideneacetone)dipalladium(0) (2.66 g, 2.92 mmol) and tri-*tert*-butylphosphine (11.2 mL of a 0.33 M solution in hexanes, 3.7 mmol) were added. The reaction was heated at 55 °C for 24 h under nitrogen and then allowed to cool to ambient temperature. The organic phase was decanted and the residue rinsed with ethyl acetate. The combined organics were evaporated, and the residue was partitioned between ethyl acetate (400 mL) and water (200 mL). The organic phase was separated, dried ($MgSO_4$), filtered, and evaporated. The residue crystallized from hot isohexane to give **22a** as a white solid (33.64 g, 90%). δ^H (500 MHz, $CDCl_3$): 7.18 (1 H, t, $J = 9.2$ Hz), 7.28 (1 H, dd, $J = 0.9$, 7.5 Hz), 7.32 (1 H, m), 7.45 (1 H, m), 7.56 (1 H, ddd, $J = 1.7$, 7.5, 9.2 Hz), 8.47 (1 H, d, $J = 2.3$ Hz); *m*/*z* (ES+) 210 (MH^+).

2-(5-Bromo-2-fluorophenyl)-3,5-difluoropyridine (23a). To **22a** (33.6 g, 160.76 mmol) in acetonitrile (330 mL) was added dibromodimethylhydantoin (1.5 equiv, 68.85 g, 240.5 mmol). The mixture was cooled to 4 °C, and concentrated sulfuric acid (51.9 mL, 6 equiv, 95.4 g, 0.974 mol) was added slowly with efficient stirring to maintain the internal temperature below 20 °C. On completion of addition, the cooling bath was removed and the mixture stirred a further 10 min at RT. The vessel was then transferred to a preheated oil bath at 55 °C and the mixture heated at 55 °C for 2 h. Most of the solvent was then stripped at reduced pressure, the residue diluted with water, and 4 N aq NaOH (310 mL) added, and the mixture extracted with isohexane. The organic phase was washed with water, separated, dried ($MgSO_4$), filtered, and evaporated and the residue chromatographed on silica, eluent 45% CH_2Cl_2 in isohexane, to give **23a** as a white solid (32.34 g, 111.9 mmol, 70%). δ^H (500 MHz, $CDCl_3$): 7.07 (1 H, t, $J = 9.2$ Hz), 7.33 (1 H, ddd, $J = 2.4$, 7.7, 8.9 Hz), 7.55 (1 H, ddd, $J = 2.7$, 4.7, 8.9 Hz), 7.72 (1 H, dd, $J = 2.6$, 6.2 Hz), 8.47 (1 H, d, $J = 2.4$ Hz); *m*/*z* (ES+) 288/290 (MH^+).

[3-(3,5-Difluoropyridin-2-yl)-4-fluorophenyl]boronic Acid (24a). To a solution of **23a** (31.34 g, 108.4 mmol) and bis(neopentylglycolato)diboron (29.6 g, 131 mmol) in dry dioxane (230 mL) was added potassium acetate (6.13 g, 230.4 mmol), and the mixture was degassed for 1 h. Dichloro[1,1′-bis(diphenylphosphino)ferrocene]palladium(II) DCM adduct (2.02 g, 2.5 mmol) was added and the mixture degassed for a further 15 min and then heated at 80 °C for 24 h. The reaction was cooled to ambient temperature, 1 M aq NaOH (1060 mL) was added, and the mixture was stirred at RT for 1 h in air. Ethyl acetate in isohexane (30%) (250 mL) was added, the mixture was stirred a further 10 min, and then the phases were separated. The aqueous layer was washed with 30% ethyl acetate in isohexane, and the combined organics were washed with water (200 mL). The combined aqueous layers were filtered through a fine filter paper and then taken to pH 4 by addition of 10 N aq HCl (∼108 mL). The mixture was allowed to get warm during the acidification and was stirred at 40 °C for 0.5 h to complete boronate hydrolysis. The mixture was then aged at RT for 2 h and the solid

collected by filtration, washed with water, and then dried in vacuo at 65 °C to afford **24a** as a white solid (26.5 g, 105 mmol, 97%). δ^H (500 MHz, DMSO-d_6): 7.33 (1 H, dd, J = 8.5, 10.5 Hz), 7.97 (1 H, m), 8.01 (1 H, dd, J = 1.5, 7.8 Hz), 8.10 (1 H, m), 8.20 (2 H, s), 8.70 (1 H, d, J = 2.3 Hz); m/z (ES+) 254 (MH^+).

5-[3-(3,5-Difluoropyridin-2-yl)-4-fluorophenyl]-2*H*-pyridazin-3-one (25a). To **24a** (26.5 g, 105 mmol), 5-chloropyridazin-3(2*H*)-one[6] (16.6 g, 127 mmol), and dioxane (500 mL) was added 2 M aqueous sodium carbonate (140 mL). The mixture was degassed by vacuum/N_2 cycles, and then dichloro[1,1′-bis(diphenylphosphino)ferrocene]palladium (II) DCM adduct (3.0 g, 3.69 mmol) was added and the mixture heated at 85 °C for 22 h under N_2. Water (500 mL) was added while still hot and the mixture stirred with cooling in an ice bath at 4 °C for 0.75 h. The solid was collected by filtration washed with water until filtrate colorless, air-dried, and then washed with isohexane. The filter cake was dried in vacuo at 60 °C to give **25a** a white solid (26.6 g, 83%). δ^H (500 MHz, DMSO-d_6): 7.17 (1 H, s), 7.55 (1 H, t, J = 9.5 Hz), 8.03 (2 H, m), 8.16 (1 H, t, J = 8.3 Hz), 8.32 (1 H, s), 8.72 (1 H, s), 13.14 (1 H, br s).

3-Chloro-5-[3-(3,5-difluoropyridin-2-yl)-4-fluorophenyl]pyridazine (26a). To phosphorus oxychloride (300 mL) preheated at 70−80 °C was added **25a** (13 g, 45.6 mmol) portionwise with stirring, and the solution was heated for 0.5 h after becoming homogeneous. Excess phosphorus oxychloride was stripped at reduced pressure and the residue azeotroped with toluene. The dark oil was treated with ice (300 g) with external ice cooling. The mixture was adjusted to pH 6 with saturated $NaHCO_3$ solution and extracted with EtOAc (2 × 300 mL). The combined organics were dried ($MgSO_4$), filtered, and evaporated to give a beige solid, which was recrystallized from hot EtOAc/isohexane (14.4 g, 98%). δ^H (500 MHz, DMSO-d_6): 7.62 (1 H, t, J = 9.2 Hz), 8.2 (3 H, m), 8.35 (1 H, d, J = 1.9 Hz), 8.74 (1 H, d, J = 2.1 Hz), 9.72 (1 H, d, J = 1.8 Hz); m/z (ES+) 322/324 (MH^+).

3-Fluoro-2-(2-fluorophenyl)pyridine (22b). 2-Fluorobenzeneboronic acid (5.32 g, 38 mmol), 2-chloro-3-fluoropyridine (5.0 g, 38 mmol), dry THF (100 mL), potassium fluoride (11.2 g, 0.193 mol), and water (3.0 mL) were combined, and the mixture was degassed by vacuum/N_2 cycles. Tris(dibenzylideneacetone)dipalladium(0) (0.776 g, 0.852 mmol) and tri-*tert*-butylphosphine (4.90 mL of a 0.33 M solution in hexanes, 1.6 mmol) were added. The reaction was heated at 55 °C for 24 h under nitrogen and then allowed to cool to ambient temperature. The organic phase was decanted and residue rinsed with ethyl acetate. The combined organics were evaporated, and the residue was chromatographed on silica, eluent CH_2Cl_2, to give **22b** as a yellow oil (6.26 g, 86%). δ^H (500 MHz, $CDCl_3$): 7.18 (1 H, t, J = 9.1 Hz), 7.28 (1 H, t, J = 7.6 Hz), 7.34 (1 H, m), 7.44 (1 H, m), 7.50 (1 H, t, J = 8.8 Hz), 7.61 (1 H, t, J = 7.2 Hz), 8.54 (1 H, s); m/z (ES+) 192 (MH^+).

2-(5-Bromo-2-fluorophenyl)-3-fluoropyridine (23b). To **22b** (6.26 g, 32.79 mmol) in acetonitrile (67 mL) was added dibromodimethylhydantoin (1.5 equiv, 14.04 g, 49 mmol). The mixture was cooled to 4 °C, and concentrated sulfuric acid (10.58 mL, 6 equiv, 0.198 mol) was added slowly with efficient stirring to maintain the internal temperature below 20 °C. On completion of addition, the cooling bath was removed and the mixture stirred a further 10 min at RT. The vessel was then transferred to a preheated oil bath at 55 °C and the mixture heated at 55 °C for 2 h. Most of the solvent was then stripped at reduced pressure and the residue neutralized by addition of 4 N aq NaOH (65 mL) with cooling in an ice water bath. The product was extracted with ethyl acetate, the organic phase was washed with water, separated, dried ($MgSO_4$), filtered, and evaporated, and the residue was chromatographed on silica, eluent 50% CH_2Cl_2 in isohexane to give **23b** as a white solid (6.12 g, 69%). δ^H (500 MHz, $CDCl_3$): 7.08 (1 H, t, J = 9.1 Hz), 7.37 (1 H, m), 7.53 (2 H, m), 7.76 (1 H, dd, J = 2.5, 6.2 Hz), 8.55 (1 H, dt, J = 1.4, 4.6 Hz); m/z (ES+) 270/272 (MH^+).

[3-(3-Fluoropyridin-2-yl)-4-fluorophenyl]boronic Acid (24b). To a solution of **23b** (6.12 g, 22.58 mmol), and bis(neopentylglycolato)diboron (6.17 g, 27.3 mmol) in dry dioxane (50 mL) was added potassium acetate (4.70 g, 176.6 mmol), and the mixture was thoroughly degassed. Dichloro[1,1′-bis(diphenylphosphino)ferrocene]palladium(II) DCM adduct (0.416 g, 0.515 mmol) was added and the mixture degassed and then heated at 80 °C for 18 h under N_2. The reaction was cooled to RT, 1 M aq NaOH (210 mL) was added, and the mixture was stirred at RT for 0.5 h in air. Diethyl ether (120 mL) was added, the mixture was stirred a further 10 min, and then the phases were separated. The aqueous layer was filtered through a fine filter paper and then taken to pH 4 by addition of 2 N aq HCl (∼117 mL). The mixture was allowed to get warm during the acidification and was stirred at 45 °C for 0.5 h to complete boronate hydrolysis. The mixture was then aged at RT for 2 h, and the solid was collected by filtration, washed with water, and then dried in vacuo at 60 °C to afford **24b** as a cream solid (5.0 g, 94%). δ^H (500 MHz, DMSO-d_6): 7.32 (1 H, dd, J = 8.4, 10.5 Hz), 7.58 (1 H, m), 7.87 (1 H, m), 7.97 (1 H, m), 8.05 (1 H, dd, J = 1.5, 7.9 Hz), 8.20 (2 H, s), 8.59 (1 H, m); m/z (ES+) 236 (MH^+).

5-[3-(3-Fluoropyridin-2-yl)-4-fluorophenyl]-2*H*-pyridazin-3-one (25b). To **24b** (5.0 g, 21.15 mmol), 5-chloropyridazin-3(2*H*)-one[6] (3.54 g, 27.08 mmol), and dioxane (88 mL) was added 2 M aqueous sodium carbonate (41 mL). The mixture was degassed by vacuum/N_2 cycles, and then dichloro[1,1′-bis(diphenylphosphino)ferrocene]palladium (II) DCM adduct (1.0 g, 1.23 mmol) was added and the mixture heated at 85 °C for 20 h under N_2. Most of the dioxane was stripped at reduced pressure, water (150 mL) was added, and the mixture was stirred at 50 °C for 0.5 h and then allowed to stand at RT for 2 h. The solid was collected by filtration washed with water, cold ethanol, and then diethyl ether. The filter cake was dried in vacuo at 60 °C to give **25b**, a white solid (5.078 g, 84%). δ^H (500 MHz, DMSO-d_6): 7.19 (1 H, s), 7.54 (1 H, t, J = 9.2 Hz), 7.62 (1 H, m), 7.92 (1 H, t, J = 9.0 Hz), 8.04 (2 H, m), 8.33 (1 H, d, J = 1.9 Hz), 8.62 (1 H, d, J = 4.3 Hz), 13.14 (1 H, s); m/z (ES+) 286 (MH^+).

3-Chloro-5-[3-(3-fluoropyridin-2-yl)-4-fluorophenyl]pyridazine (26b). To phosphorus oxychloride (100 mL) preheated at 70−80 °C was added **25b** (5.078 g, 17.81 mmol) portionwise with stirring, and the solution was heated for 0.5 h after becoming homogeneous. Excess phosphorus oxychloride was stripped at reduced pressure and the residue azeotroped with toluene. The dark oil was treated with ice (100 g) with external ice cooling. The mixture was adjusted to pH 6 with saturated $NaHCO_3$ solution and the resulting solid collected by filtration, washed with water, and then dried in vacuo at 60 °C (4.66 g, 86%). δ^H (500 MHz, DMSO-d_6): 7.63 (2 H, m), 7.94 (1 H, m), 8.22 (1 H, m), 8.26 (1 H, dd, J = 2.4, 6.7 Hz), 8.36 (1 H, d, J = 1.9 Hz), 8.63 (1 H, m), 9.73 (1 H, d, J = 1.9 Hz); m/z (ES+) 304/306 (MH^+).

Representative Suzuki Coupling. 5-[3-(3,5-Difluoropyridin-2-yl)-4-fluorophenyl]-3-(2-fluorophenyl)pyridazine (8). To **26a** (0.2 g, 0.62 mmol) and 2-fluorophenylboronic acid (0.131 g, 0.93 mmol) in dioxane (3 mL) was added sodium carbonate solution (2 N, 1 mL) followed by tetrakistriphenylphosphinepalladium(0) (36 mg; 31 μmol), and the mixture was heated at 150 °C in a Smith microwave reactor for 600 s. The reaction was diluted with dioxane (20 mL), separated, and evaporated onto silica gel. The crude product was chromatographed on silica eluting on a gradient with 50% to 100% ethyl acetate in isohexane to give **8** as a white solid (149 mg, 63% yield). δ^H (500 MHz,$CDCl_3$): 7.20−7.24 (1 H, m), 7.34−7.41 (3 H, m), 7.47−7.53 (1 H, m), 7.80−7.84 (1 H, m), 7.96 (1 H, dd, J = 2.3, 6.7 Hz), 8.13 (1 H, t, J = 2.0 Hz), 8.19−8.24 (1 H, m), 8.52 (1 H, d, J = 2.3 Hz), 9.44 (1 H, d, J = 2.0 Hz); m/z (ES+) 382 (MH^+). Acc Mass ($C_{21}H_{11}F_4N_3$) requires: 382.0962, found: 382.0950 Da.

5-[3-(3,5-Difluoropyridin-2-yl)-4-fluorophenyl]-3-(4-fluorophenyl)pyridazine (6). Prepared in the same manner as **8** by Suzuki reaction. δ^H (500 MHz, $CDCl_3$): 7.42 (2 H, t, J = 9.0 Hz), 7.62 (1 H, dd, J = 8.6, 0.8 Hz), 8.17−8.22 (1 H, m), 8.27−8.39 (4 H, m), 8.55 (1 H, d, J = 2.3 Hz), 8.75 (1 H, d, J = 2.3 Hz), 9.66 (1 H, d, J = 2.3 Hz); m/z (ES+) 382 (MH^+). Anal. ($C_{21}H_{11}F_4N_3$. 0.5(H_2O)) C, H, N.

5-[4-Fluoro-3-(3-fluoropyridin-2-yl)phenyl]-3-(2-fluorophenyl)-pyridazine (7). Prepared in the same manner as **8** via Suzuki

reaction. δ^H (500 MHz, $CDCl_3$): 7.41−7.46 (2 H, m), 7.53−7.66 (3 H, m), 7.91−8.02 (2 H, m), 8.20−8.27 (2 H, m), 8.37 (1 H, t, J = 2.0 Hz), 8.63−8.64 (1 H, m), 9.72 (1 H, d, J = 2.3 Hz); m/z (ES+) 364 (MH^+). Acc Mass ($C_{21}H_{12}F_3N_3$) requires: 364.1062, found: 364.1060 Da.

3-(2,4-Difluorophenyl)-5-[3-(3,5-difluoropyridin-2-yl)-4-fluorophenyl]pyridazine (9). Prepared in the same manner as **8** by Suzuki reaction. δ^H (400 MHz, $CDCl_3$): 6.96−7.02 (1H, m), 7.08−7.13 (1H, m), 7.36−7.42 (2H, m), 7.79−7.83 (1H, m), 7.95 (1H, dd, J = 2.3, 6.3 Hz), 8.09 (1H, t, J = 2.2 Hz), 8.23−8.29 (1H, m), 8.52 (1H, d, J = 2.3 Hz), 9.44 (1H, d, J = 2.3 Hz); m/z (ES+) 400 (MH^+). Anal. ($C_{21}H_{10}F_5N_3$. 0.4(H_2O)) C, H, N.

Representative Reverse Stille Coupling. 3-(2,6-Difluorophenyl)-5-[4-fluoro-3-(3-fluoropyridin-2-yl)-phenyl]pyridazine (10). To a degassed mixture of **26b** (0.25 g, 0.82 mmol), hexamethylditin (0.323 g, 0.98 mmol), and lithium chloride (0.1024 g, 2.46 mmol) in 1,4-dioxane (12 mL) was added tetrakis(triphenylphosphine)-palladium(0) (0.048 g, 0.041 mmol), and the mixture was heated at 100 °C for 3 h. Mass spectroscopy showed formation of stannane **36**. 1-Bromo-2,6-difluorobenzene (0.3177 g, 0.187 mL, 1.65 mmol) was added, followed by tetrakis(triphenylphosphine) palladium(0) (0.01 g, 0.0082 mmol), and the mixture was heated at 100 °C for 6 h. The reaction was cooled to RT, filtered, and evaporated, and the crude product was chromatographed on silica, eluent 4% methanol−CH_2Cl_2, to give **10** which was recrystallized from ethyl acetate/isohexane as a white solid (42 mg, 14%). δ^H (400 MHz, $CDCl_3$) 7.05−7.12 (2 H, m), 7.32−7.59 (4 H, m), 7.79−7.85 (2 H, m), 8.00 (1 H, dd, J = 2.5, 6.5 Hz), 8.58−8.60 (1 H, m), 9.51 (1 H, d, J = 2.3 Hz); m/z (ES+) 382 (MH^+). Anal. ($C_{21}H_{11}F_4N_3$. 0.5(H_2O)) C, H, N.

Representative Stille Coupling. 5-[4-Fluoro-3-(3,5-difluoropyridin-2-yl)-phenyl]-3-(3,5-difluoropyridin-4-yl)pyridazine (14). To **26a** (0.2 g; 0.62 mmol) and 3,5-difluoro-4-trimethylstannylpyridine (0.35 g, 1.26 mmol) in dioxane (3 mL) were added copper(I) iodide (6 mg, 0.03 mmol) and lithium chloride (0.026 g, 0.62 mmol) followed by tetrakis(triphenylphosphine)palladium(0) (71 mg, 62 μmol), and the mixture was heated at 100 °C for 18 h. The reaction was diluted with DCM (20 mL) and the organic layer separated, dried over $MgSO_4$, filtered, and evaporated. Chromatography on silica eluted with 7% ethyl acetate in isohexane gave **14** as a white solid (115 mg, 46% yield). Crystallized from hot ethyl acetate. Mp 199−201 °C. δ^H (500 MHz, DMSO-d_6): 7.65 (1 H, m), 8.16 (1 H, ddd, J = 2.4, 9, 9 Hz), 8.24−8.26 (2 H, m), 8.53 (1 H, br s), 8.74 (1 H, d, J = 2.2 Hz), 8.81 (2 H, s), 9.87 (1 H, d, J = 2.3 Hz); m/z (ES+) 401 (MH^+). Anal. ($C_{20}H_9F_5N_4$) C, H, N.

5-[4-Fluoro-3-(3-fluoropyridin-2-yl)-phenyl]-3-(3-fluoropyridin-4-yl)pyridazine (11). Prepared in the same manner as **14** by Stille procedure: δ^H (500 MHz, $CDCl_3$) 7.42 (2 H, m), 7.58 (1 H, t, J = 8.9 Hz), 7.83 (1 H, m), 8.01 (1 H, dd, J = 2.4, 6.5 Hz), 8.22 (2 H, m), 8.60 (1 H, m), 8.64 (1 H, d J = 5 Hz), 8.67 (1H, d, J = 2 Hz), 9.54 (1 H, d, J = 2.0 Hz); m/z (ES+) 365 (MH^+). Acc Mass ($C_{20}H_{11}F_3N_4$) requires: 365.0951, found: 365.0945 Da.

5-[3-(3,5-Difluoropyridin-2-yl)-4-fluorophenyl]-3-(3-fluoropyridin-4-yl)pyridazine (12). Prepared in the same manner as **14** by Stille procedure: δ^H (400 MHz, $CDCl_3$) 7.36−7.44 (2 H, m), 7.81−7.85 (1 H, m), 7.97 (1 H, dd, J = 2, 7 Hz), 8.21−8.24 (2 H, m), 8.52 (1 H, d, J = 2 Hz), 8.64−8.68 (2 H, m), 9.53 (1 H, d, J = 2 Hz); m/z (ES^+) 383 (MH^+). Acc Mass ($C_{20}H_{10}F_4N_4$) requires: 383.0914, found: 383.0960 Da.

3-(3,5-Difluoropyridin-4-yl)-5-[4-fluoro-3-(3-fluoropyridin-2-yl)phenyl]pyridazine (13). Prepared in the same manner as **14** by Stille procedure. Crystallized from hot 2-propanol by addition of water: δ^H (500 MHz, DMSO-d_6) 7.62−7.66 (2 H, m), 7.94 (1 H, br t, J = 9.2 Hz), 8.23−8.27 (2 H, m), 8.54 (1 H, br s), 8.63 (1 H, br d, J = 4.5 Hz), 8.80 (2 H, s), 9.88 (1 H, d, J = 2.2 Hz); m/z (ES+) 383 (MH^+). Anal. ($C_{20}H_{10}F_4N_4$) C, H, N.

5-[4-Fluoro-3-(3-fluoropyridin-2-yl)-phenyl]-3-(3,5-difluoropyridin-2-yl)pyridazine (15). Prepared in the same manner as **14** by Stille procedure. δ^H (500 MHz, DMSO-d_6) 7.60−7.66 (2 H, m), 7.93 (1 H, br t, J = 9.2 Hz), 8.21−8.25 (3 H, m), 8.48 (1 H, d, J = 2.2 Hz), 8.64 (1 H, br d, J = 4.6 Hz), 8.76 (1 H, d, J = 2.1 Hz), 9.80 (1 H, d, J = 2.2 Hz); m/z (ES+) 383 (MH^+). Anal. ($C_{20}H_{10}F_4N_4$. 0.45(H_2O)) C, H, N.

5-[3-(3,5-Difluoropyridin-2-yl)-4-fluorophenyl]-3-(2,4,6-trifluorophenyl)pyridazine (17). Prepared by the same method as **10.** δ^H (500 MHz, $CDCl_3$) 6.86 (2 H, t, J = 8.2 Hz), 7.34−7.41 (2 H, m), 7.81 (2 H, t, J = 6.4 Hz), 7.94 (1 H, dd, J = 2.2, 6.4 Hz), 8.51 (1 H, d, J = 2.2 Hz), 9.47−9.57 (1 H, m).; m/z (ES^+) 418 (MH^+). Anal. ($C_{21}H_9F_6N_3$. 0.4(H_2O)) C, H, N.

5-[4-Fluoro-3-(3-fluoropyridin-2-yl)-phenyl]-3-(3-fluoropyridin-2-yl)pyridazine (18). Prepared in the same manner as **14** by Stille proceedure: δ^H (400 MHz, $CDCl_3$) 7.35−7.48 (3 H, m), 7.55−7.61 (1 H, m), 7.63−7.68 (1 H, m), 7.84−7.89 (1 H, m), 8.05 (1 H, dd, J = 3, 7 Hz), 8.41 (1 H, d, J = 2 Hz), 8.58−8.62 (2 H, m), 9.54 (1 H, d, J = 2 Hz); m/z (ES^+) 365 (MH^+). Acc Mass. $C_{20}H_{11}F_3N_4$ requires: 365.1014, found: 365.0993 Da.

5-[3-(3,5-Difluoropyridin-2-yl)-4-fluorophenyl]-3-(3-fluoropyridin-2-yl)pyridazine (19). Prepared in the same manner as **14** by Stille proceedure: δ^H (500 MHz, $CDCl_3$) 7.36−7.41 (2 H, m), 7.46−7.49 (1 H, m), 7.66 (1 H, t, J = 10 Hz), 7.85−7.89 (1 H, m), 8.01 (1 H, dd, J = 2, 7 Hz), 8.41 (1 H, s), 8.52 (1 H, s), 8.61 (1 H, d, J = 4 Hz), 9.53 (1 H, s); m/z (ES^+) 383 (MH^+). Anal. ($C_{20}H_{10}F_4N_4$) C, H, N.

Representative Negishi Coupling. 5-[4-Fluoro-3-(3,5-difluoropyridin-2-yl)-phenyl]-3-(3,5-difluoropyridin-2-yl)pyridazine (16). To a stirred solution of TMEDA (7.04 g; 60.6 mmol) in dry diethyl ether (120 mL) at −78 °C under a N_2 atmosphere was added *n*-butyllithium (58.6 mmol; 23.5 mL of 2.5 M in hexanes), and the mixture was stirred for 15 min. **30** (10.59 g, 56.57 mmol) was then added dropwise over 10 min and then the reaction aged for 1.5 h. Zinc chloride (61 mmol, 61 mL of 1 M in diethyl ether) was added over 15 min and the mixture stirred at −78 °C for 1 h and then allowed to warm to −10 °C to afford **33**. The chloropyridazine **26a** (13.00 g, 40.41 mmol) was added as a solid, followed by dichloro[1,1′-bis(diphenylphosphino)ferrocene]palladium(II) DCM adduct (1.32 g, 1.62 mmol) and dry THF (150 mL). The mixture was then heated at reflux for 6 h. The reaction was concentrated to half volume, DMA (15 mL) was added, followed by KF (5.0 g, 86 mmol), and the reaction was heated at 60 °C for 1 h to complete desilylation. On cooling, the reaction was treated with water (500 mL) containing EDTA (100 g) and NaOH (35 g), and the mixture was vigorously stirred for 0.5 h and then extracted with CH_2Cl_2 (2 × 500 mL). The organic phase was separated, washed with water, dried ($MgSO_4$) filtered, and evaporated onto silica. Chromatography on silica, gradient eluent CH_2Cl_2 to 40% ethyl acetate in CH_2Cl_2, gave **16**, which was dissolved in hot methanol (700 mL) and then boiled with activated charcoal (5 g) for 1 h. The mixture was filtered hot through GF/A filter paper, and the filtrate was concentrated to 100 mL and then allowed to stand at RT. The solid was collected by filtration and dried in vacuo, to afford **16** as a pale yellow solid (9.0 g, 56%). δ^H (500 MHz, DMSO-d_6): 7.61−7.65 (1 H, m), 8.16−8.24 (4 H, m), 8.48 (1 H, s), 8.75 (2 H, d, J = 12.2 Hz), 9.79 (1 H, s).; m/z (ES+) 401 (MH^+). Anal. ($C_{20}H_9F_5N_4$. 0.5(H_2O)) C, H, N.

3,5-Difluoro-4-trimethylstannanylpyridine (29). To a solution of *N*,*N*,*N*′,*N*′-tetramethylethylenediamine (3.85 g, 5 mL, 33.13 mmol) in dry ether (100 mL) at −78 °C was added *n*-butyllithium (10.0 mL, 25 mmol, 2.5 M in hexanes), and the mixture was stirred at −35 °C for 1 h and then cooled to −78 °C. A solution of 3,5-difluoropyridine **27** (2.63 g, 22.8 mmol) in dry ether (8 mL) was added and the mixture stirred for 2 h. Trimethyltin chloride (25 mL, 25 mmol, 1 M solution in hexane) was added and the mixture stirred at −78 °C for 1 h and allowed to warm to RT. The reaction was then cooled to −78 °C and quenched by the addition of water (5 mL). After being warmed to RT, the organic phase was separated, dried ($MgSO_4$), filtered, and evaporated. The crude product was purified by dry flash chromatography on silica eluted with 10% ethyl acetate in isohexane, to give **29** as a yellow oil (1.67 g, 26%). δ^H (400 MHz, $CDCl_3$) 8.22 (2 H, s), 0.48 (9 H, s).

3,5-Difluoro-4-trimethylsilanylpyridine (30). A solution of *n*-butyllithium (250 mmol, 100 mL of 2.5 M in hexanes) was added

via a cannula to a solution of TMEDA (34.57 g, 297.5 mmol) in diethyl ether (400 mL) at −78 °C, and the solution was stirred for 0.5 h. A solution of 3,5-difluoropyridine (27.39 g, 238 mmol) in diethyl ether (100 mL) was then added via a cannula, and the resulting mixture was stirred at −78 °C for 2 h, before adding chlorotrimethylsilane (33 mL, 262 mmol) The solution stirred for 0.5 h and then allowed to warm to RT over 2 h. The reaction was quenched into water (500 mL), and the organic phase was separated, washed with 10% aqueous citric acid, water, dried ($MgSO_4$), and evaporated. The residue was distilled at reduced pressure to give **30** as a colorless oil (bp 62 °C @ 5 mbar), (30 g, 67%). δ^H (400 MHz, $CDCl_3$) 8.24 (2 H, s), 0.41 (9 H).

3,5-Difluoro-4-trimethylsilanyl-2-trimethylstannanylpyridine (32). To a solution of 3,5-difluoropyridine (3.0 g, 26.01 mmol) in diethyl ether (100 mL) at −78 °C was added lithium diisopropylamide (13.7 mL, 27.4 mmol, 2 M solution in THF), and the solution was stirred for 0.5 h. Chlorotrimethylsilane (2.95 g, 3.47 mL, 27.15 mmol) was added and the solution stirred for 0.5 h and then allowed to warm to RT and stirred for 1 h. The solution was then cooled to −78 °C, a solution of lithium diisoproylamide (13.7 mL, 27.4 mmol, 2 M solution in THF) was added, and the solution was stirred for 0.5 h. Trimethyltin chloride (28.7 mL, 28.7 mmol, 1 M in hexanes) was added and the solution stirred for 0.5 h and then allowed to warm to RT over 18 h. The mixture was diluted with isohexane (100 mL) and poured into water (200 mL). The organic phase was washed with water (3 × 200 mL) and then dried over $MgSO_4$, filtered, and evaporated to give an orange oil. Purification by distillation at reduced pressure gave a pale yellow oil (7.4 g, 81%; bp 110 °C 1.3 mmHg). δ^H (400 MHz, $CDCl_3$) 8.42 (1 H, s), 0.39 (9 H, s), 0.38 (9 H, s).

Acknowledgment. We thank Sarah Kelly for the synthesis of compound **30**, and Drs. Angus M MacLeod, Leslie J. Street, José L. Castro, and Ruth M. Mckernan for useful discussions.

Supporting Information Available: Table S1 contains analytical or accurate mass data for compounds **6**−**19**. This material is available free of charge via the Internet at http://pubs.acs.org.

References

(1) Simon, J.; Wakimoto, H.; Fujita, N.; Lalande, M.; Barnard, E. A. Analysis of the set of GABAA Receptor Genes in the Human Genome. *J Biol. Chem.* **2004**, *279*(40), 41422−41435. (b) Atack, J. R. The benzodiazepine binding site of $GABA_A$ receptors as a target for the development of novel anxiolytics. *Expert Opin. Investig. Drugs* **2005**, *14*(5), 601−618. See also: Whiting, P. J. The GABA-A receptor gene family: New opportunities for drug development. *Curr. Opin. Drug Discovery Dev.* **2003**, *6*(5), 648−657, and references therein. (c) The γ3 subtype is of low abundance in mammalian brain. In this work only the γ2 subtype combination has been studied in vitro. Knoflach, F.; Rhyner, Th.; Villa, M.; Kellenberger, S.; Drescher, U.; Malherbe, P.; Sigel, E.; Mohler, H. The γ3-subunit of the $GABA_A$-receptor confers sensitivity to benzodiazepine receptor ligands. *FEBS Lett.* **1991**, *293*(1−2), 191−194; see also: Baer, K.; Essrich, C.; Benson, J.; Benke, D.; Bluethmann, H.; Fritschy, J.-M.; Luscher, B. Postsynaptic clustering of γ-aminobutyric acid type A receptors by the γ3 subunit in vivo. *Proc. Natl. Acad. Sci. U.S.A.* **1999**, *96*(22), 12860−12865.

(2) Low, K.; Crestani, F.; Keist, R.; Benke, D.; Brunig, I.; Benson, J. A.; Fritschy, J. M.; Rulicke, T.; Bluethmann, H.; Mohler, H.; Rudolph, U. Molecular and neuronal substrate for the selective attenuation of anxiety. *Science* **2000**, *290*(5489), 131−134, and references therein.

(3) McKernan, R. M.; Rosahl, T. W.; Reynolds, D. S.; Sur, C.; Wafford, K. A.; Atack, J. R.; Farrar, S.; Myers, J.; Cook, G.; Ferris, P.; Garrett, L.; Bristow, L.; Marshall, G.; Macaulay, A.; Brown, N.; Howell, O.; Moore, K. W.; Carling, R. W.; Street, L. J.; Castro, J. L.; Ragan, C. I.; Dawson, G. R.; Whiting, P. J. *Nature Neurosci.* **2000**, *3*(6), 587−592, and references therein. (b) Atack, J. R.; Wafford, K. A.; Tye, S. J.; Cook, S. M.; Sohal, B.; Pike, A.; Sur, C.; Melillo, D.; Bristow, L.; Bromidge, F.; Ragan, C. I.; Kerby, J.; Street, L. J.; Carling, R. W.; Castro, J. L.; Whiting, P. J.; Dawson, G. R.; McKernan, R. M. TP A023, An Agonist Selective for α2- and α3-Containing $GABA_A$ Receptors is a Nonsedating Anxiolytic in Rodents and Primates. *J. Pharmacol. Exp. Ther.* **2006**, *316*, 410−422, and references therein. (c) See also ref 6. (d) Dias, R.; Sheppard, W. F.; Fradley, R. L.; Garrett, E. M.; Stanley, J. L.; Tye, S. J.; Goodacre, S.; Lincoln, R. J.; Cook, S. M.; Conley, R.; Hallett, D.; Humphries, A. C.; Thompson, S. A.; Wafford, K. A.; Street, L. J.; Castro, J. L.; Whiting, P. J.; Rosahl, T. W.; Atack, J. R.; McKernan, R. M.; Dawson, G. R.; Reynolds, D. S. Evidence for a significant role of α3-containing $GABA_A$ receptors in mediating the anxiolytic effects of benzodiazepines. *J. Neurosci.* **2005**, *25*(46), 10682−10688.

(4) Unpublished results from these laboratories. This observation is based upon examination of more than 10 chemically distinct structural classes. The γ2 subunit (the most abundant γ subtype in CNS), which is held invariant in these studies, makes significant contributions to the binding pocket. Furthermore the α subunits are highly homologous, and the modest binding selectivity achievable for α2/α3 over α1 may be attributable to a single amino acid residue difference which is isoleucine in α3 and valine in α1 (P. Wingrove, personal communication). For published studies on the molecular determinants of subtype selective binding affinity, see also: Pritchett, D. B.; Seeburg, P. H. γ-Aminobutyric acid type A receptor point mutation increases the affinity of compounds for the benzodiazepine site. *Proc. Natl. Acad. Sci. U.S.A.* **1991**, *88*, 1421−1425. Korpi, E. R.; Grunder, G.; Luddens, H.; Drug interactions at $GABA_A$ receptors. *Prog. Neurobiol.* **2002**, *67*, 113−159.

(5) Chambers, M.; Atack, J.; Carling, R.; Collinson, N.; Cook, S.; Dawson, G.; Ferris, P.; Hobbs, S.; O'Connor, D.; Marshall, G.; Rycroft, W.; MacLeod, A. An Orally Bioavailable, Functionally Selective Inverse Agonist at the Benzodiazepine Site of $GABA_A$ α5 Receptors with Cognition Enhancing Properties. *J. Med. Chem.* **2004**, *47*(24), 5829−5832 and references therein.

(6) Van Niel, M. B.; Wilson, K.; Adkins, C. H.; Atack, J. R.; Castro, J. L.; Clarke, D. E.; Fletcher, S.; Gerhard, U.; Mackey, M. M.; Malpas, S.; Maubach, K.; Newman, R.; O'Connor, D.; Pillai, G. V.; Simpson, P. B.; Thomas, S. R.; MacLeod, A. M. A New Pyridazine Series of $GABA_A$ α5 ligands. *J. Med. Chem.* **2005**, *48*, 6004−6011.

(7) Russell, M. G. N.; Carling, R. W.; Street, L. J.; Hallett, D. J.; Mezzogori, E.; Atack, J. R.; Cook, S. M.; Bromidge, F. A.; Wafford, K. A.; Marshall, G. R.; Reynolds, D. S.; Stanley, J.; Lincoln, R.; Tye, S. J.; Sheppard, W. F. A.; Sohal, B.; Pike, A.; Dominguez, M.; Castro, J. L. Discovery of Imidazo[1,2-*b*][1,2,4]triazines as $GABA_A$ α2/3 Subtype Selective Agonists for the Treatment of Anxiety. *J. Med. Chem.* **2006**, *49*(4), 1235−1238. (b) Carling, R. W.; Madin, A.; Guiblin, A.; Russell, M. G. N.; Moore, K. W.; Mitchinson, A.; Sohal, B.; Pike, A.; Cook, S. M.; Ragan, I.C.; McKernan, R. M.; Quirk, K.; Ferris, P.; Marshall, G. R.; Thompson, S. A.; Wafford, K. A.; Dawson, G. R.; Atack, J. R.; Harrison, T.; Castro, J. L.; Street, L. J.; 7-(1,1-Dimethylethyl)-6-(2-ethyl-2*H*-1,2,4-triazol-3-ylmethoxy)-3-(2-fluorophenyl)-1,2,4-triazolo[4,3-*b*]pyridazine: A Functionally Selective $GABA_A$ α2/α3-Subtype Selective Agonist which Exhibits Potent Anxiolytic Activity but is Not Sedating in Animal Models. *J. Med. Chem* **2005**, *48*, 7089−7092. (c) Goodacre, S. G.; Street, L. J.; Hallett, D. J.; Crawforth, J. M.; Kelly, S.; Owens, A. P.; Blackaby, W. P.; Lewis, R. T.; Stanley, J.; Smith, A. J.; Ferris, P.; Sohal, B.; Cook, S. M.; Pike, A.; Teall, M.; Wafford, K. A.; Marshall, G. R.; Castro, J. L.; Atack, J. R.; Imidazo[1,2-*a*]pyrimidines as Functionally Selective and Orally Bioavailable $GABA_A$ α2/α3 Binding Site Agonists for the Treatment of Anxiety Disorders. *J. Med. Chem.* **2006**, *49*(1), 35−38. (d) Jennings, A. S. R.; Lewis, R. T.; Russell, M. G. N.; Hallett, D. J.; Crawforth, J.; Street, L. J.; Castro, J. L.; Atack, J. R.; Cook, S. M.; Lincoln, R.; Stanley, J.; Smith, A. J.; Reynolds, D. S.; Sohal, B.; Pike, A.; Marshall, G. R.; Wafford, K. A. Imidazo[1,2-*b*][1,2,4]triazines as α2/α3 subtype selective $GABA_A$ agonists for the treatment of anxiety. *Bioorg. Med. Chem. Lett.* **2006**, *16*(6), 1477−1480.

(8) Unpublished results from these laboratories. For example, the hydroxydimethyl moiety of **2**, a key feature of the imidazotriazine series, was not well tolerated as a 3-substituent in the pyridazine series: Ar = $(CH_3)_2COH$, R= H K_i α3 226 nM.

(9) The α2 binding affinity was not routinely measured. It closely parallels the α3 affinity for those compounds studied; **16**: K_i α2 10.91 nM; K_i α3 8.5 nM and **17**: K_i α2 4.6 nM; K_i α3 5.0 nM.

(10) A combination of HPLC-MS-MS. analysis of the material recovered after incubation with rat hepatocytes.

(11) The protocol for these assays has been published elsewhere. See ref 3 and references therein for experimental protocols for rat in vivo occupancy, plus-maze, and rotarod assays in the presence or absence of coadministered ethanol, and primate CER.

(12) It is important to note that occupancy of all BZ receptor subtypes is measured[11] by the test compound's ability to displace tritiated Ro 15-1788, but that the efficacy derives only from occupancy of those native receptors containing α2 or α3 for this compound.

(13) Compound **14** possesses no significant off target activities at 1000 times its effective anxiolytic plasma concentration, as assessed in a 'MDS Pharma screen where it was assayed against a panel of 170 enzyme, G-protein-coupled receptor, ion channel, and amino acid transporter receptors. MDS Pharma Services, Taiwan Ltd., Pharmacology Laboratories, 158 Li-Teh Road, Peitou, Taipei, Taiwan 112, R. O. C.

(14) Littke, A. F.; Fu, G. C. Palladium-Catalysed Coupling Reactions of Aryl Chlorides. *Angew. Chem., Int. Ed.* **2002**, *41*, 4176−4211, and references therein.

(15) Eguchi, H.; Kawaguchi, H.; Yoshinaga, S.; Nishida, A.; Nishiguchi, T.; Fujisaka, S. Halogenation using N-halogeno compounds. II. Acid-catalyzed bromination of aromatic compounds with 1,3-dibromo-5,5-dimethylhydantoin. *Bull. Chem. Soc. Jpn.* **1994**, *67*(7), 1918−1921. (b) Olah, G. A.; Wang, Q.; Sandford, G.; Surya, P. G. K. Synthetic methods and reactions 181. Iodination of deactivated aromatics with *N*-iodosuccinimide in trifluoromethanesulfonic acid. *J. Org. Chem.* **1993**, *58*(11), 3194−3195.

(16) Ishiyama, T.; Itoh, Y.; Kitano, T.; Miyaura, N. Synthesis of arylboronates via the palladium(0)-catalyzed cross-coupling reaction of tetra(alkoxo)diborons with aryl triflates. *Tetrahedron Lett*. **1997**, *38*(19), 3447−3450.

(17) Queguiner, G.; Marsais, F. Review on the Metallation of π-deficient Heteroaromatic Compounds. *Tetrahedron* **1983**, *39*(12), 2009−2021. (b) Gros, P.; Choppin, S.; Mathieu, J.; Fort, Y. Lithiation of 2-heterosubstituted Pyridines *J. Org. Chem*. **2002**, *67*, 234−237. (c) See also Chambers, R. D.; Hall, C. W.; Hutchinson, J.; Millar, R. W. Polyhalogenated heterocyclic compounds. Part 42. Fluorinated nitrogen heterocycles with unusual substitution patterns. *J. Chem. Soc., Perkin Trans. 1* **1998**, (10), 1705−1713.

(18) 2-Bromo-3,5-difluoropyridine **21a** may be prepared by the action of $AlBr_3$ and HBr on 2,3,5-trifluoropyridine by adaptation of the method of Chambers et al. in ref 17c for the preparation of 2,4,6-tribromo-3,5-difluoropyridine from pentafluoropyridine.

JM051144X